Journal of Materials Chemistry A

ROYAL SOCIETY OF CHEMISTRY

PAPER

Cite this: *J. Mater. Chem. A*, 2020, **8**, 15034

Ionic liquid polymer materials with tunable nanopores controlled by surfactant aggregates: a novel approach for CO_2 capture†

Ambavaram Vijaya Bhaskar Reddy,[a] Muhammad Moniruzzaman, *[ab] Mohamad A. Bustam,[ab] Masahiro Goto,[c] Bidyut B. Saha[d] and Christoph Janiak *[e]

Received 28th November 2019
Accepted 7th July 2020

DOI: 10.1039/c9ta13077b

rsc.li/materials-a

Monomeric ionic liquids (ILs), ionic liquid polymers (ILPs) and IL-based composites have emerged as potential materials for CO_2 capture owing to their exceptional intrinsic physical solubility of CO_2. This study reports the development of novel IL polymer materials incorporating CO_2-philic tunable nanopores and their subsequent utilization for CO_2 capture. In this approach, primarily, micelles were formed in monomeric IL 1-vinyl-3-ethylimidazolium bis(trifluoromethylsulfonyl)imide using a CO_2-philic surfactant (*N*-ethyl perfluorooctyl sulfonamide) through self-assembly, from which polymeric materials were fabricated *via* free radical polymerization. The CO_2 adsorption studies demonstrated 3-fold enhancements for the surfactant micelle incorporated IL polymers (SMI-ILPs) compared to their bare IL polymers. The SMI-ILPs were regenerated by simply heating at 70 °C and reused for 15 cycles with a retention of over 96% of CO_2 uptake capacity. The simple recovery and notable enhancements in CO_2 sorption of novel SMI-ILPs were traced to the adsorption of CO_2 at the (i) highly porous IL-based polymeric networks, and (ii) nanometer sized apolar pores made by CO_2-philic surfactant tails. This work will open up new possibilities for the development of IL based smart materials for CO_2 capture and separation.

Introduction

The Kyoto protocol was established to monitor and control the emissions of greenhouse gases (GHGs). Although, progress has been made in reducing GHG emissions over the past two decades, it is still becoming progressively imperative to find methods to capture CO_2.[1] Therefore, in response to the Kyoto protocol, the development and discovery of advanced materials with accompanying processes that can selectively and efficiently capture CO_2 is crucial and still remains challenging. The current leading technologies involving aqueous alkanolamine solutions have several limitations such as being highly corrosive and energy intensive with volatile amine losses.[2,3] Subsequently, there is an increasing demand for the development of innovative, efficient, non-volatile, non-corrosive and eco-friendly materials for the selective separation and capture of CO_2.

In recent years, ionic liquid (IL) technology has gained attention owing to its acceptable thermal stability, low vapour pressure, low volatility, reusability and exceptional CO_2 solubility. The initial examination of CO_2 solubility in IL[bmim][PF_6] was reported by Blanchard *et al.*, in 1999.[4] Afterwards, vast research has been conducted to ascertain the solubility of CO_2 in a wide range of ILs.[5,6] In conventional ILs, the solubility of CO_2 proceeds by solvation through weak intermolecular forces. But the slow rate of CO_2 diffusion across bulk liquids is a major drawback associated with the conventional ILs. The diffusion rates of CO_2 across the room temperature ILs are up to 19 times slower than those with standard amines.[7] The slow diffusion of CO_2 through conventional ILs prevents rapid sorption and requires substantial energy for the recycle/regeneration of ILs. One potential solution to overcome the above problem is the polymerization of ILs.[8] IL polymers composed of covalently linked IL species offer the features of macromolecules. The sorption efficiency of such IL polymers significantly outperforms the sorption efficiency of corresponding monomeric ILs

[a]*Centre of Research in Ionic Liquids, Universiti Teknologi PETRONAS, Seri Iskandar 32610, Perak, Malaysia. E-mail: m.moniruzzaman@utp.edu.my*

[b]*Department of Chemical Engineering, Universiti Teknologi PETRONAS, Seri Iskandar 32610, Perak, Malaysia*

[c]*Department of Applied Chemistry and Centre for Future Chemistry, Kyushu University, 744 Motooka, Nishi-ku, Fukuoka 819-0395, Japan*

[d]*International Institute for Carbon-Neutral Energy Research (WPI-I2CNER), Department of Mechanical Engineering, Graduate School of Engineering, Kyushu University, 744 Motooka, Nishi-ku, Fukuoka 819-0395, Japan*

[e]*Institute of Inorganic and Structural Chemistry, Heinrich-Heine-University, 40204 Düsseldorf, Germany. E-mail: janiak@uni-duesseldorf.de*

† Electronic supplementary information (ESI) available: Characterization of the IL monomer and polymers, the CMC of the surfactant in [veim][Tf_2N]–chloroform, NMR, FTIR, and SEM-EDX spectra, sorption isotherms, pore size distributions, adsorption capacity, isosteric heat, and data tables. See DOI: 10.1039/c9ta13077b

due to their improved processability, enhanced stability, durability and better control over their meso- to nano-structures.[9–11] Current efforts involve the design of IL polymers with high surface areas, high porosity, low density, and high thermal and chemical stability to support energy efficient CO_2 separation processes.[12–15] A variety of supports typically silica, activated carbon, zeolites, metal–organic frameworks, covalent organic frameworks, porous organic polymers, conjugated microporous polymers and porous aromatic frameworks have been tested for this purpose in combination with the selected ILs.[16–18] Besides, IL polymer composite membranes exhibited higher CO_2 solubility and faster sorption/desorption rates compared to IL monomers and IL polymers.[19,20]

Here, we have prepared surfactant micelle incorporated IL polymers (SMI-ILPs) to enhance the CO_2 sorption efficiency owing to the higher encapsulation capacity of CO_2-philic micelles. Although, a few studies reported the formation of surfactant micelles in IL monomers for enzymatic applications,[21,22] the formation of SMI-ILPs and their application for enhanced CO_2 capture are new. The surfactant, *N*-ethyl perfluorooctyl sulfonamide, was used for the micelle formation due to its fluorooctyl groups, which have a high affinity for CO_2.[23] The IL monomer, 1-vinyl-3-ethylimidazolium bis(trifluoromethylsulfonyl)imide [veim][Tf_2N], was selected due to its good affinity with CO_2, relatively low melting point, and low viscosity as well as its simple preparation.[24] A schematic representation for the formation of SMI-ILPs is presented in Fig. 1. Overall, we believe that the high reusability and relatively high CO_2 sorption of novel SMI-ILPs provide opportunities for developing sustainable SMI-ILPs to address the global CO_2 problems.

Results and discussion

The size and formation of surfactant micelles in the [veim][Tf_2N]–chloroform (1.0 : 0.1, wt%) mixture were determined by dynamic light scattering (DLS), and their subsequent incorporation into the lattice structure of IL polymers was confirmed by Fourier transform infrared spectroscopy (FTIR), scanning electron microscopy (SEM), energy-dispersive X-ray (EDX) analysis and elemental mapping. The thermophysical characterization of SMI-ILPs was performed using thermogravimetric analysis (TGA), and porosity analysis by nitrogen sorption and Brunauer–Emmett–Teller (BET) evaluation. The CO_2 sorption mechanism was assessed using the heat of sorption and FTIR analysis before and after CO_2 sorption.

Initially, the structural analysis of the synthesized IL monomer [veim][Tf_2N] was carried out using ^1H NMR and ^{13}C NMR spectroscopy. The spectral data that confirmed the synthesis and purity of the IL monomer are presented in Fig. S1, ESI.† The viscosity and density of the prepared [veim][Tf_2N] in the presence of chloroform (10 wt%) were found to be 48.038 mPa s and 1.504 g cm^{-3} at 25 °C, respectively. Micelles with varying sizes were formed in the [veim][Tf_2N]–chloroform mixture upon addition of the surfactant between 0.1% and 10% (wt%). The solubility of the surfactant and progression in micelle formation were observed by adding chloroform as the co-solvent. However, the other tested polar solvents including ethanol and methanol only molecularly dissolved the surfactant without forming micelles, and mid non-polar solvents including hexane and diethyl ether precipitated the surfactant instead of forming micelles. Although, the addition of other ILs such as [emim][Tf_2N] and [emim][Ac] improved the micelle formation, the polymerization process became tricky as they contain no polymerizable groups. The DLS data of surfactant micelles in the [veim][Tf_2N]–chloroform mixture disclosed that the average hydrodynamic diameter of the micelles increased from 30 nm to 340 nm in accordance with the surfactant fraction from 0.1% to 10% (w/w) as presented in Fig. 2. This indicates that the attractive forces between the micelles have led to the increase in the micelle size on addition of the surfactant.[25] However,with the addition of more than 3.0 wt% surfactant, the

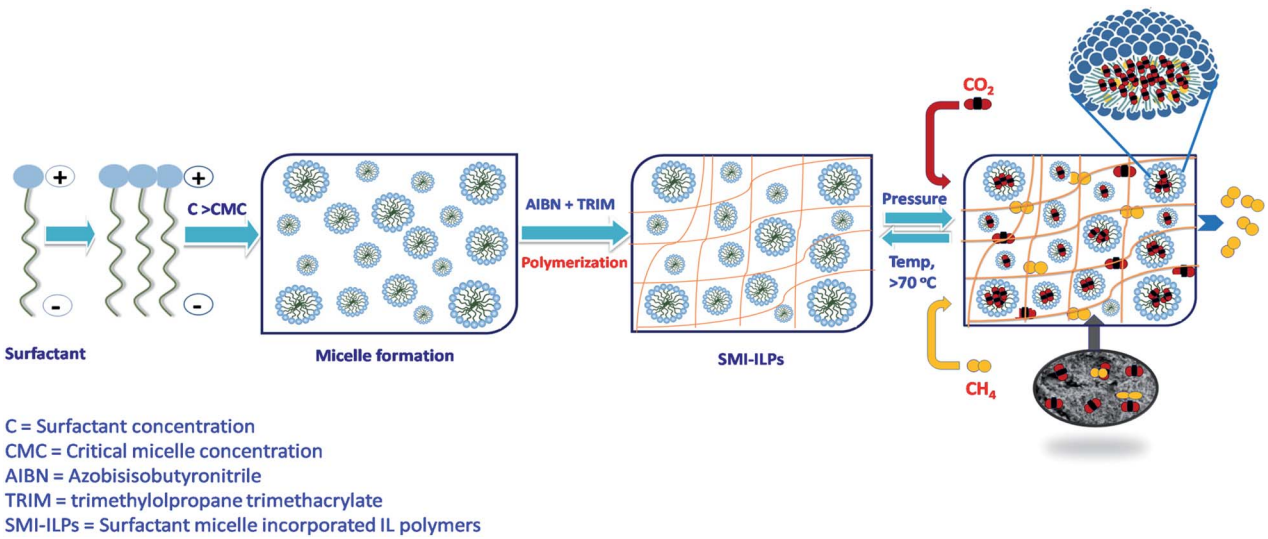

Fig. 1 Schematic representation for the formation of surfactant micelles and their subsequent incorporation into IL polymers.

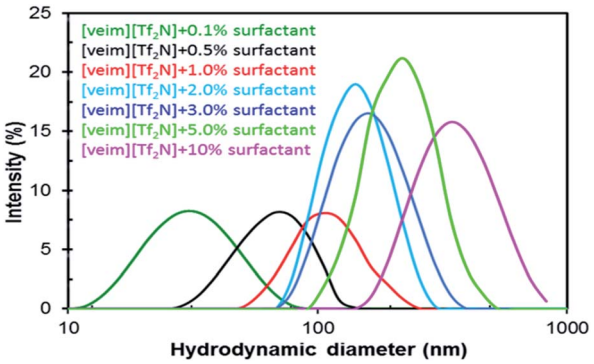

Fig. 2 Typical size distribution of micelles in the IL–chloroform solution at different surfactant concentrations measured by DLS.

aggregate size was greatly increased and vesicles were anticipated to form. The increased polydispersity index (PDI) (>0.6) of the micelles with the surfactant fraction (>3.0 wt%) in the IL–chloroform mixture indicates a broad size distribution of micelles with different sizes. The critical micelle concentration (CMC) of the surfactant in the IL–chloroform mixture was found to be 0.001 wt% (8×10^{-3} mol L^{-1}) at 25 °C (Fig. S2, ESI†). Therefore, the surfactant concentration for the micelle formation in the [veim][Tf_2N]–chloroform mixture was considered from 0.1 wt%, which is considerably higher than the CMC.

The presence of the surfactant and incorporation of surfactant micelles into poly[veim][Tf_2N] were supported by the identification of surfactant functional groups in FTIR analysis, although most of the functional groups of the surfactant and IL polymer are similar and hence it is critical to distinguish the FTIR spectra of the surfactant from those of the IL polymer. The corresponding FTIR spectra of the surfactant, poly[veim][Tf_2N] and SMI-poly[veim][Tf_2N] are shown in Fig. 3. A peak that appeared at 3313 cm^{-1} for SMI-poly[veim][Tf_2N] is the characteristic peak of the surfactant that corresponds to the N–H stretching of the amide group. Similarly, the peaks that appeared at 3144 cm^{-1} and 2980 cm^{-1} represent the alkene C–H stretching of the imidazolium ring of the polymer and surfactant respectively. Further, the peaks that appeared at 1050 cm^{-1} and 1348 cm^{-1} are due to the SO_2 symmetric and asymmetric stretching respectively. Additionally, the peaks at 1126 cm^{-1} and 1178 cm^{-1} are characteristic of the C–F stretching of both the polymer and surfactant. The strong vibration bands between 1200 and 1500 cm^{-1} are characteristic peaks of the Tf_2N anion. At last, the peak at 1729 cm^{-1} corresponds to the C═O group of trimethylolpropane trimethacrylate (TRIM).

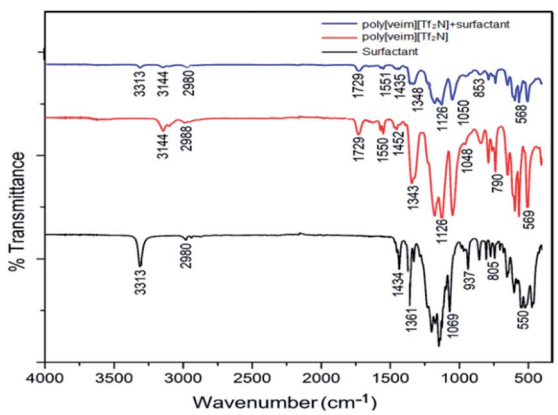

Fig. 3 FTIR spectra of the surfactant (black), poly[veim][Tf_2N] (red) and SMI-poly[veim][Tf_2N] (blue).

The polydispersity index (PDI) of the synthesized SMI-ILPs containing <3.0 wt% surfactant was found to be below 0.5. Therefore, materials containing <3.0 wt% surfactant possess narrow MWD and provide good mechanical properties. However, the high PDI (>0.6) of the materials with increasing surfactant fraction (>3.0 wt%) in the IL–chloroform mixture indicated broad size distributions of micelles with different sizes.

To assess the homogeneity of IL polymer materials, the crystallization behavior of poly[veim][Tf_2N] and 10 wt% SMI-poly[veim][Tf_2N] was analysed using DSC (Fig. S3†). The crystallization temperature of poly[veim][Tf_2N] was found to be 93.5 °C, which shifted to 96.5 °C in the case of 10 wt% SMI-ILP. This shift indicates that the surfactant micelles act as nucleation centers for the crystallization of poly[veim][Tf_2N] and incorporating micelles into the IL polymer increases the crystallization temperature.[26,27] The crystallization processes were finished within 1.0 °C which is a good indication of the homogeneous character of both the poly[veim][Tf_2N] and SMI-poly[veim][Tf_2N] materials.[28]

SEM analysis revealed varying sizes and distinct morphologies for the different SMI-poly[veim][Tf_2N] materials as presented in Fig. 4. Bare poly[veim][Tf_2N] displayed a rough surface with a negligible porous structure. In contrast, the SMI-poly[veim][Tf_2N] materials showed virtually homogeneous round shaped micelles with an enhanced porous surface, in which the micelle sizes were in good agreement with the DLS observations. Also, the micrographs at higher magnifications disclosed that the surfactant micelles were capsulized into the micropores of poly[veim][Tf_2N] and resulted in spherical shaped porous materials with increased porosity. The surfactant addition at a lower weight percentage produced spherical micelles with a uniform size as shown in Fig. 4b–d. In contrast, on addition of high surfactant amounts (>2.0 wt%), the resulting micelles were agglomerated and not well separated, so "Ostwald ripening" growth can be presumed as shown in Fig. 4e–h, where the transformation of the micelle morphology from spherical to ellipsoidal particles and the subsequen evolvution to entangled cuboids were observed.

Further, EDX elemental mapping of poly[veim][Tf_2N] and SMI-poly[veim][Tf_2N] materials confirmed the incorporation of micelles and their uniform distribution in poly[veim][Tf_2N] as presented in Fig. S4, ESI,† with the elemental composition varying in accordance with the surfactant micelle incorporation (Table S1, ESI†). Next, the N_2 adsorption–desorption measurements (Fig. S5, ESI†) showed that while poly[veim][Tf_2N] is little porous, the surface area and pore volume of poly[veim][Tf_2N] materials increased up to 228 m^2 g^{-1} from 27 m^2 g^{-1} and 0.42 cm^3 g^{-1} from 0.14 cm^3 g^{-1} with 1.0 wt% surfactant micelle

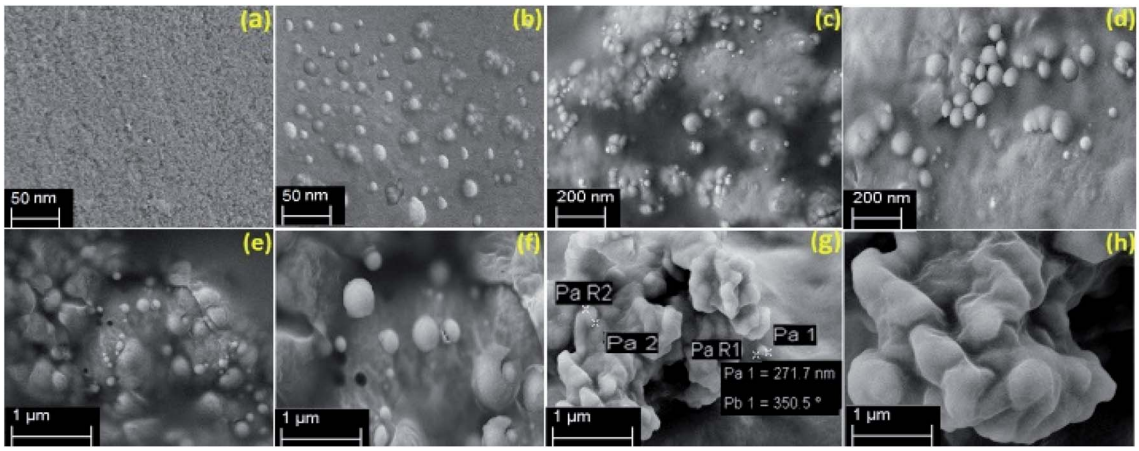

Fig. 4 SEM images of (a) poly[veim][Tf_2N] and SMI-poly[veim][Tf_2N] with the addition of (b) 0.1 wt%, (c) 0.5%, (d) 1.0 wt%, (e) 2.0 wt%, (f) 3.0 wt%, (g) 5.0 wt% and (h) 10 wt% surfactant.

incorporation (Table S2, ESI†). As shown in Fig. S5, ESI,† the samples with 0.1 wt% and 1.0 wt% surfactant micelle incorporation showed Type-IV isotherms with H2 hysteresis loops that are typical characteristics of mesoporous materials. As a result, the surface area and pore size distributions were increased with the increase of the surfactant weight percentage from 0.1% to 1.0% in IL polymers. However, with the addition of above 1.0 wt% surfactant, the surface area and porosity decreased again owing to the formation of aggregate vesicles.

Thermogravimetric analysis (TGA) showed that a significant weight loss of over 10%, indicative of decomposition of poly[veim][Tf_2N] materials, only occured around 350 °C (Fig. 5). From TGA it can be found that the SMI-poly[veim][Tf_2N] materials are largely free of solvent and moisture as there was no significant weight loss at temperatures below 250 °C. However, the materials with above 1.0% surfactant micelle incorporation started to experience an earlier onset of the polymer decomposition.

CO_2 sorption measurements indicated a steady increase in CO_2 uptake with increasing pressure from 1.0 bar to 20 bar for both poly[veim][Tf_2N] and its SMI-poly[veim][Tf_2N] composites (Fig. 6 and S6, ESI†). The surfactant micelle incorporation into polymer materials significantly enhanced the CO_2 uptake. With 1.0 wt% surfactant, nearly 3-fold enhancements were recorded for CO_2 uptake in all pressure ranges (Table S3, ESI†). However, when the surfactant amount exceeded 1.0 wt%, the CO_2 sorption decreased again, probably due to the formation of large aggregates in the form of vesicles. The highest CO_2 sorption was found to be 41 mmol g^{-1} for 1.0 wt% SMI-poly[veim][Tf_2N] at 298 K temperature and 20 bar pressure. The other expected rationale is that the addition of the surfactant increased the fluoromethyl and amine group contents that are exceptionally CO_2-philic. The formation of micelles with high specific surface areas and pore volumes was expected to be the prime factor accountable for higher sorption capacities. Additionally, the incorporation of an additional fluorine content in the form of surfactant micelles will be advantageous for CO_2 sorption. Porous structures with a great number of micelles are known to contain potential adsorption sites for CO_2 molecules.[29]

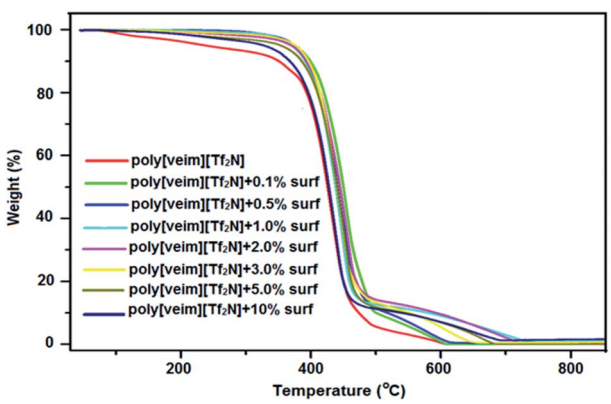

Fig. 5 Representative TGA thermograms for different SMI-poly[veim][Tf_2N] materials recorded at 10 °C min^{-1} heating rate under a N_2 atmosphere. The few percent weight loss below 350 °C is due to the vaporization of residual water.

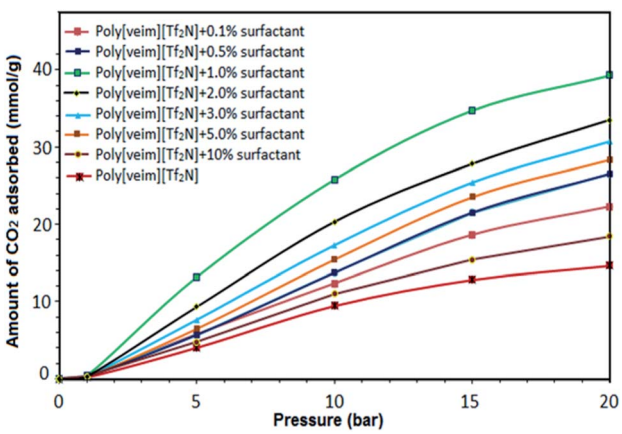

Fig. 6 Representative CO_2 adsorption isotherms of different SMI-poly[veim][Tf_2N] materials at 298 K and varying pressures between 1.0 and 20 bar.

Physical CO_2 adsorption is the dominant process, as FTIR spectroscopy indicated no changes in the materials before and after the adsorption experiments (Fig. S7†). Further, it was clear that the sulfonyl and carbonyl functionalities are not sufficient to enhance the CO_2 adsorption; the fluoroalkyl groups in [Tf_2N] played a key role in the adsorption of CO_2. ILs with anions containing fluoroalkyl groups were found to have some of the highest CO_2 adsorption capacities and as the quantity of fluoroalkyl groups increased, the CO_2 adsorption capacity was also increased. These results are in good agreement with the reported literature, wherein the authors concluded that ILs or ILPs containing increased fluoroalkyl chains on either cations or anions improve the CO_2 solubility and selectivity when compared to less fluorinated ILPs.[30,31] A free volume mechanism, where CO_2 molecules were introduced into the free spaces/cavities of polymerized ILs, is permissible. Moreover, the long fluoroalkyl chain of the surfactant increased the van der Waals interactions between CO_2 and SMI-ILPs and provided relatively higher adsorption. Besides, the selected surfactant contains active fluoroalkyl groups and a secondary amine that helps to enhance the CO_2 uptake and selectivity, not by only forming micelles. In addition, the SMI-poly[veim][Tf_2N] composites were found to be thermally and chemically stable at higher temperatures. However, increasing the fluorination level to an even greater extent decreased the CO_2 adsorption capacity by decreasing the microporosity and pore volume of the polymers. These results are in good agreement with the reported studies, where the authors noticed low CO_2 adsorption for highly fluorinated compounds over non-fluorinated samples.[32–34] Therefore, an optimized weight percentage of surfactant utilized in the micelle formation has confirmed its ability for higher CO_2 sorption. Nevertheless, the specific surface area and pore volume are other important parameters that can influence the CO_2 sorption capacity of ILP materials.[35] As shown in Table S2,† the specific surface area and pore volume of SMI-ILPs were increased to 228 $m^2\ g^{-1}$ and 0.42 $cm^3\ g^{-1}$ respectively with increasing the surfactant micelle incorporation to 1.0 wt%. Accordingly, the highest CO_2 sorption capacity of 41.31 mmol g^{-1} was found with the SMI-ILPs containing 1.0 wt% surfactant. Therefore, the high CO_2 sorption capacity of SMI-ILPs with 1.0 wt% surfactant is mainly associated with their high specific surface area and pore volume. Overall, the results conclude that the incorporation of surfactant micelles provided large specific surface areas and pore volumes, a tunable pore size and stability, which have had substantial influence on the sorption capacity of the resulting SMI-ILPs.

Next, the increase of the isosteric heat of adsorption and the decrease of activation energy barriers from poly[veim][Tf_2N] to 1.0 wt% SMI-poly[veim][Tf_2N] indicated the higher adsorption capacity for CO_2 of the SMI-poly[veim][Tf_2N] material over the bare poly[veim][Tf_2N] material. The heat of adsorption (Q_{st}) at low coverage of poly[veim][Tf_2N] was found to be around 30 kJ mol^{-1}. However, the incorporation of the CO_2-philic surfactant enhanced the interactions between the resultant SMI-ILP and CO_2 molecules and provided a higher heat of adsorption value at a low coverage of 40 kJ mol^{-1} for 1.0 wt% SMI-ILPs (Fig. S8, ESI†). The Q_{st} values gradually decreased and flattened as the CO_2 molecules occupied more surface active sites.

Further, selective adsorption of CO_2 from a mixture of gases (*e.g.*, CO_2–CH_4) is highly desirable in natural gas purification. Hence, we have checked CH_4 adsorption of the synthesized SMI-ILPs, and the results for the poly[veim][Tf_2N] and SMI-poly[veim][Tf_2N] materials are presented in Fig. S9 (ESI†). As can be seen, there is no significant difference in CH_4 adsorption for all different SMI-ILPs, and the adsorption was found between 2.0 and 2.5 mmol g^{-1}. Therefore, it is anticipated that surfactant micelle incorporation has no influence on CH_4 adsorption. The slight differences in CH_4 adsorption among poly[veim][Tf_2N] and SMI-poly[veim][Tf_2N] materials can be traced to the varying specific surface areas and pore volumes of the materials. Unlike the CO_2 adsorption results, surfactant micelles did not support the SMI-ILPs to increase the CH_4 adsorption. However, the high specific surface area and pore volume of 1.0 wt% SMI-ILPs provided infinitesimally higher CH_4 adsorption. Hence, CH_4 adsorption studies confirmed the preferential adsorption capacity of SMI-ILPs for CO_2 over CH_4.

In addition, the multicycle ad/desorption of CO_2 in poly[veim][Tf_2N] and SMI-poly[veim][Tf_2N] (1.0 wt%) materials is presented in Fig. 7. From the data, it can be observed that the SMI-poly[veim][Tf_2N] material retained over 96% of its high CO_2 capacity at a constant temperature of 70 °C even after 15 consecutive cycles, which is not possible for other industrially used chemical sorbents (MEA/H_2O only recovered 82% capacity at 120 °C temperatures).[36] The SMI-poly[veim][Tf_2N] material was successfully regenerated by simply heating it at 70 °C without applying any pressure. Hence, the synthesized SMI-poly[veim][Tf_2N] materials possess excellent recyclability and require less energy than the bare IL polymers and aqueous amine systems for their recovery (Table S4, ESI†). The simple reusability of SMI-poly[veim][Tf_2N] is mainly due to its physisorption, and hence CO_2 molecules can desorb at only moderately elevated temperature or reduced pressure; however in amine solutions (MEA/H_2O) CO_2 capture proceeds through chemisorption and formation of carbamates. Particularly in the SMI-poly[veim][Tf_2N] material, the CO_2 molecules stick to the pore walls and produce a continuous chain along the edges of

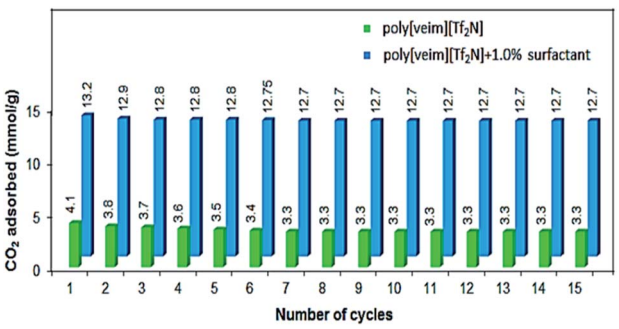

Fig. 7 Reusability of poly[veim][Tf_2N] and its 1.0 wt% SMI-poly[veim][Tf_2N] material, where adsorption was performed at 25 °C and 5.0 bar pressure, and desorption was performed at 70 °C temperature and 1.0 bar pressure.

mesopores. As a result, the CO_2 molecules adsorbed at the pore walls readily desorb only at moderately elevated temperature. It is also evidenced from the calculated isosteric heats of adsorption (Q_{st}) as presented in Fig. S8, ESI.† In addition, water tolerance of these SMI-poly[veim][Tf_2N] materials is an added advantage since the gas molecules always contain moisture and many commercial sorbents are not stable in the presence of water.

Experimental

Materials

The surfactant *N*-ethyl perfluorooctyl sulfonamide, bromoethane and 1-vinylimidazole were purchased from Sigma Aldrich, USA (≥99% purity). 1-Ethyl-3-methylimidazolium acetate and bis(trifluoromethane)sulfonimide lithium were also obtained from Sigma Aldrich, USA (≥99.99% purity). All received chemicals were of the highest purity available and consumed without additional purification. Further, a free radical initiator 2,2′-azobis(2-methylpropionitrile) (AIBN) was obtained from R & M chemicals and reagents, Malaysia, and it was recrystallized with methanol before its application in the polymerization process. The cross linker trimethylolpropane trimethacrylate (TRIM) was obtained from Sigma Aldrich, USA (≥98% purity). All solvents including chloroform, ethanol, methanol, toluene, acetonitrile, ethyl acetate and diethyl ether were obtained from Merck and were of analytical grade with ≥99% purity. The solutions were prepared by weighing the compounds with a Sartorius®-CP124S competence series of a laboratory balance. To prevent hydration, the ILs were kept in tightly closed vials and placed in a desiccator before use, and they were manipulated inside a glove box under a dry nitrogen atmosphere. The water content in ILs was analyzed using a Karl Fischer titrator (Mettler Toledo KF DL31) and NMR technique (Bruker DRX-500 spectrometer); the reported estimations were lower than 200 ppm in all cases.

Synthesis of [veim][Br] and [veim][Tf_2N] monomers

Initially, the IL monomer 1-vinyl-3-ethylimidazolium bromide [veim][Br] was prepared by adding 33 g of 0.3 mol L^{-1} bromoethane dropwise into a double neck round bottom flask containing 28 g of 0.3 mol L^{-1} 1-vinylimidazole under vigorous stirring in an ice bath followed by heating at 40 °C for 2 h. At the end of the reaction, a white precipitate was formed at the bottom, and it was washed with ethyl acetate several times to ensure the removal of unreacted materials from the final product. Subsequently, the product was dried on a rotary evaporator at a reduced pressure and temperature of 50 mbar and 60 °C respectively, followed by freeze-drying for 24 h. The yield obtained after freeze-drying was found to be 45.6 g (~97%).

Next, the IL monomer 1-vinyl-3-ethylimidazolium bis(trifluoromethylsulfonyl)imide [veim][Tf_2N] was synthesized by ion exchange between the IL monomer [veim][Br] and bis(trifluoromethylsulfonyl)imide lithium salt [LiTf_2N] considering a molar ratio of 1 : 1.1 respectively. In this approach, 12.8 g of 0.06 mol L^{-1} [veim][Br] was weighed into a double neck round bottom flask and dissolved in 6.0 mL of distilled water. Next, 18.9 g of 0.066 M LiTf_2N was weighed accurately and added dropwise into the round bottom flask to minimize the heat generated. The mixture was then stirred continuously at ambient temperature until the formation of a two-phase system containing [veim][Tf_2N] at the bottom phase and aqueous LiBr at the top phase. Subsequently, the bottom phase of [veim][Tf_2N] was separated and washed several times with distilled water and dried with a rotary evaporator operating at 75 °C temperature and 50 mbar pressure to ensure the removal of unreacted compounds dissolved in water. Both the IL monomers were stored in a desiccator until further use to avoid the water absorption.

Micelle formation and subsequent polymerization

Surfactant micelles were formed in the [veim][Tf_2N]–chloroform (1.0 : 0.1; wt%) mixture with varying sizes by adding different amounts of surfactant between 0.1% and 10% (wt%) with constant stirring at 360 rpm for about 2 h at 40 °C. Additionally, the effect of other solvents including ethanol, methanol and acetonitrile, and other ILs such as [emim][Tf_2N] and [emim][Ac] on the size and formation of micelles in [veim][Tf_2N] was examined. Afterwards, the surfactant micelle incorporated [veim][Tf_2N] polymers were prepared through conventional free radical polymerization. Briefly, 1.0 g of the [veim][Tf_2N] monomer containing surfactant micelles was taken in a double neck round bottom flask and purged with N_2 for 15 min. Then, 20 mg of 0.12 M AIBN and 50 mg of 0.15 M TRIM were added to the above mixture and purged again for 10 min. Eventually, the mixture was stirred vigorously under an inert atmosphere at 65 °C for 45 min to obtain a hard-elastic gel type material, which was then poured into distilled water to precipitate SMI-poly[veim][Tf_2N]. The resulting SMI-ILPs were washed with water and dried in a vacuum oven at 75 °C for 36 h and kept in a desiccator until further use. Similarly, a blank, poly[veim][Tf_2N], was also prepared without incorporating the surfactant micelles.

Micelle characterization

Initially, the viscosity and density measurements were carried out for IL monomer [veim][Tf_2N] using Anton Paar's DMA 4500 M density meter at 25 °C. Thereafter, the mean size and size distribution of surfactant micelles dispersed in the [veim][Tf_2N]–chloroform mixture were observed by DLS using a Malvern Zetasizer Nano-ZS90 (Malvern Instruments Ltd., UK) equipped with a solid-state He–Ne laser. The wavelength of the incident beam was fixed at 632.8 nm and the scattering angle was fixed at 173 °C. To ensure the temperature homogeneity of the samples, each sample was equilibrated at 25 °C for 180 s. The measurements were conducted to determine the size distribution profiles of micelles in the IL–chloroform mixture. Also, the stability of surfactant micelles has been evaluated conveniently by DLS through analyzing the samples at periodic intervals. To ensure the reproducibility of results, each run was conducted in triplicate. All solutions were filtered through

cellulose acetate membranes of 0.22 μm pore size (Millipore, USA) prior to DLS analysis.

Further, the surface tension of the [veim][Tf_2N]–chloroform mixture was measured at 25 ± 1.0 °C using a Kruss drop shape analyzer-DSA25 apparatus. This instrument obtains spatial coordinates of a drop edge, including the shape and size from which the surface tension can be determined. Measurements were performed until steady values of the surface tension appeared. The surface tension of pure water (Millipore, 18 MΩ) was utilized for the calibration. The CMC of the micelles was estimated by surface tension measurements. Briefly, different amounts of the surfactant *i.e.*, 0.005%, 0.01%, 0.05%, 0.1%, 0.5%, and 1.0% (as wt%) were dispersed in the [veim][Tf_2N]–chloroform mixture and the surface tension values at 25 °C were measured. The CMC values were determined from the inflection points on the surface tension *versus* micelle concentration curves.

Characterization of the IL monomer and polymeric materials

The ^1H NMR and ^{13}C NMR data for the synthesized [veim][Tf_2N] monomer were collected using a Bruker Avance DRX-400 spectrometer operating at 400 MHz with deuterated methanol as the solvent. The residual Br^- present in the IL monomer [veim][Tf_2N] was analysed by using a Metrohm Model 761 compact ion chromatograph (IC). The IC was equipped with a Metrosep A Supp 5–150 (6.10006.520) (4.0 mm × 150 mm) analytical column and a Metrosep A Supp 4/5 guard column (4.0 mm × 5 mm). The eluent used was a mixture of 3.2 mmol L^{-1} Na_2CO_3 and 1.0 mmol L^{-1} $NaHCO_3$. The data were analysed with the aid of Metrodata IC Net 2.3 software.

The surface morphology of the synthesized SMI-poly[veim][Tf_2N] materials was recorded on a ZEIS SUPRA TM 55VP field emission scanning electron microscope (FE-SEM), where the samples were coated uniformly on an aluminum stub having a 3.0 nm gold coating to act as a conducting material. A PerkinElmer differential scanning calorimeter DSC-Q2000 equipped with an Intracooler II was used for the examination of the crystallization properties of the synthesized materials. N_2 (99.999% purity) was employed as the purge gas. Prior to analysis, about 3–5 mg of the sample were weighed into alumina pans and heated from 25 to 110 °C at 10 °C min^{-1} to remove traces of moisture. Further, the FTIR spectra of the surfactant, poly[veim][Tf_2N] and SMI-poly[veim][Tf_2N] materials were recorded using a Shimadzu IR-Tracer-100 equipped with a diamond ATR module in the mid region of 4000–600 cm^{-1}. In addition, the FTIR spectra of ILPs and SMI-ILPs were recorded before and after CO_2 capture experiments to evaluate the sorption mechanism between CO_2 and the synthesized SMI-ILPs. All SMI-ILPs were thermally characterized by thermal gravimetric analysis (TGA, PerkinElmer, TGA 4000). The samples were cut into small pieces and heated from 50 °C to 850 °C at 10 °C min^{-1} heating rate with inert N_2 flushed at 20 mL min^{-1} to avoid the interference of corrosive gases that may cause thermal oxidative degradation. The surface area and pore size distribution of the prepared poly[veim][Tf_2N] and SMI-poly[veim][Tf_2N] materials were investigated on a Tristar II 3020 (Micromeritics, USA) surface area analyzer by means of N_2 adsorption at 77 K. Prior the adsorption experiments, the samples were pretreated at 90 °C for 30 min and then degassed at 120 °C under vacuum for 10 h. Brunauer–Emmett–Teller (BET) theory was used to calculate the specific surface areas of all the synthesized polymer materials.

CO_2 and CH_4 sorption measurements

The CO_2 sorption measurements were performed by a pressure-decay technique using a dual chamber gas sorption cell. The major components of the apparatus include a gas reservoir, thermostat, pressure gauge, isochoric cell and vacuum pump. The sorption apparatus is fully controlled using a Dell computer using an ASEPTEC Sorption DAQ system with spider (python 3.6) software, which allows precise control over the weight, pressure and temperature measurements that are necessary to determine gas absorption–desorption isotherms. The poly[veim][Tf_2N] and SMI-poly[veim][Tf_2N] materials were tested for CO_2 solubility using a gas sorption cell at a constant temperature of 298 K while the partial pressure of CO_2 increased stepwise from 1.0 bar to 20 bar. In a typical experiment, an exactly weighted amount of the polymer substance was introduced into the isochoric cell which was evacuated for about 45 min to remove any traces of gas present in the sample cell. Once the temperature and pressure were stable, CO_2 (air liquid/99.998%) was introduced into the sorption chamber, and the pressure drop was recorded until the cell's pressure remained stable for 2.0 h. The moles of CO_2 captured by the polymer substance were calculated from the difference between the initial and final number of moles of gas using eqn (1) and (2). The amount of gas adsorbed by a sample is denoted as W_{CO_2}/g. The efficiency of CO_2 sorption capacity of different IL polymers has been measured at different pressures *viz.*, 1.0, 5.0, 10, 15 and 20 bar.

$$n_{CO_2} = \frac{P_{ini}\, V_{tot}}{Z_{ini} R T_{ini}} - \frac{P_{eq}\left(V_{tot} - V_{sample}\right)}{Z_{eq} R T_{eq}} \quad (1)$$

$$W_{CO_2} = \frac{n_{CO_2} M}{W_s} \quad (2)$$

where n_{CO_2} is the moles of CO_2 captured, P_{ini} is the initial pressure, V_{tot} is the total volume of the system, Z_{ini} is the compressibility factor ($P_{ini} \times T_{ini}$), Z_{eq} is the compressibility factor ($P_{eq} \times T_{eq}$), P_{eq} is the equilibrium pressure, V_{sample} is the sample volume, $R = 0.0821$ atm L mol^{-1} K^{-1}, T_{ini} is the initial temperature, and T_{eq} is the equilibrium temperature.

Similarly, the CH_4 sorption experiments were performed using the same conditions as described above.

Conclusions

In summary, we have successfully developed new SMI-poly[veim][Tf_2N] materials and demonstrated their potential for CO_2 adsorption at varying pressures. The incorporation of surfactant micelles into IL polymers enhanced the specific surface area and the interactions of SMI-ILPs with CO_2 molecules. The presence of a large mesopore volume in SMI-ILPs led to an at

least eight-fold higher specific CO_2 adsorption under mild operating conditions compared to existing IL-based materials (Table S4†). This study provides opportunities to design and synthesize a new class of SMI-ILPs that are potentially capable of capturing CO_2 from the natural gas pre-combustion feed and from post combustion effluent gases. The formation of SMI-poly [veim][Tf_2N] is the first-ever concept with promising characteristics for future industrial applications. These novel materials could offer both low-cost and high capacity CO_2 capture and push research related to CO_2 capture and storage to new frontiers. We believe that this new SMI-ILP approach will contribute to the development of CO_2 capture technology more efficiently in the foreseeable future. In fact, IL-poly-IL materials have been used significantly in membrane technology for gas separation.[37] Since, the newly developed SMI-ILPs provided promising CO_2 sorption, they could be employed to fabricate SMI-ILP membranes that can capture and separate CO_2 from a gas mixture selectively, more efficiently and cost-effectively than currently available membrane technologies.

Conflicts of interest

Authors declared no competing financial interest.

Acknowledgements

The authors are grateful to the Universiti Teknologi Petronas for providing financial support in the form of Y-UTP grant (0153AA-E35). The authors would like to acknowledge Mr Aqeel Ahmad for his assistance in CH_4 sorption measurements.

References

1 J. E. Zafrilla, L. A. Lopez, M. A. Cadarso and O. Dejuan, *Energy Policy*, 2012, **51**, 708–719.
2 J. Yang, H. Y. Tan, Q. X. Low, B. P. Binks and J. M. Chin, *J. Mater. Chem. A*, 2015, **3**, 6440–6446.
3 P. Luis, *Desalination*, 2016, **380**, 93–99.
4 L. A. Blanchard, D. Hancu, E. J. Beckman and J. F. Brennecke, *Nature*, 1999, **399**, 28–29.
5 X. Luo and C. Wang, *Curr. Opin. Green Sustain. Chem.*, 2017, **3**, 33–38.
6 M. Aghaie, N. Rezaei and S. Zendehboudi, *Renewable Sustainable Energy Rev.*, 2018, **96**, 502–525.
7 C. Moya, J. Palomar, M. Gonzales-Miquel, J. Bedia and F. Rodriguez, *Ind. Eng. Chem. Res.*, 2014, **53**, 13782–13789.
8 Y. S. Ye, J. Rick and B. J. Hwang, *J. Mater. Chem. A*, 2013, **1**, 2719–2743.
9 X. Zhou, J. Weber and J. Yuan, *Curr. Opin. Green Sustain. Chem.*, 2019, **16**, 39–46.
10 E. D. Bates, R. D. Mayton, I. Ntai and J. H. Davis, *J. Am. Chem. Soc.*, 2002, **124**, 926–927.
11 Z. W. Liu and B. H. Han, *Curr. Opin. Green Sustain. Chem.*, 2019, **16**, 20–25.
12 K. Kumar and A. Kumar, *J. Phys. Chem. C*, 2018, **122**, 8216–8227.
13 W. Wang, M. Zhou and D. Yuan, *J. Mater. Chem. A*, 2017, **5**, 1334–1347.
14 S. Pal, A. Bhunia, P. P. Jana, S. Dey, J. Möllmer, C. Janiak and H. P. Nayek, *Chem. - Eur. J.*, 2015, **21**, 2789–2792.
15 S. Dey, A. Bhunia, H. Breitzke, P. B. Groszewicz, G. Buntkowsky and C. Janiak, *J. Mater. Chem. A*, 2017, **5**, 3609–3620.
16 D. E. Demirocak, M. K. Ram, S. S. Srinivasan, D. Y. Goswami and E. K. Stefanakos, *J. Mater. Chem. A*, 2013, **1**, 13800–13806.
17 D. Dietrich, C. Licht, A. Nuhnen, S. P. Hofert, L. De Laporte and C. Janiak, *ACS Appl. Mater. Interfaces*, 2019, **11**, 19654–19667.
18 A. Pal, M. S. Raja Shahrom, M. Moniruzzaman, C. D. Wilfred, S. Mitra, K. Thu and B. B. Saha, *Chem. Eng. J.*, 2017, **326**, 980–986.
19 Y. Zhou, W. Zhang, L. Ma, Y. Zhou and J. Wang, *ACS Sustainable Chem. Eng.*, 2019, **7**, 9387–9398.
20 Q. Zhao, P. Zhang, M. Antonietti and J. Yuan, *J. Am. Chem. Soc.*, 2012, **134**, 11852–11855.
21 M. Moniruzzaman, N. Kamiya, K. Nakashima and M. Goto, *ChemPhysChem*, 2008, **9**, 689–692.
22 M. Moniruzzaman, N. Kamiya, K. Nakashima and M. Goto, *Green Chem.*, 2008, **10**, 497–500.
23 D. B. Key, R. D. Howell and C. S. Criddle, *Environ. Sci. Technol.*, 1997, **31**, 2445–2454.
24 A. Blasig, J. Tang, X. Hu, S. P. Tan, Y. Shen and M. Radosz, *Ind. Eng. Chem. Res.*, 2007, **46**, 5542–5547.
25 M. E. Parent, J. Yang, Y. Jeon, M. F. Toney, Z. L. Zhou and D. Henze, *Langmuir*, 2011, **27**, 11845–11851.
26 C. Xing, L. Zhao, J. You, W. Dong, X. Cao and Y. J. Li, *J. Phys. Chem. B*, 2012, **116**, 8312–8320.
27 C. Liu, K. W. Chan, J. Shen, C. Z. Liao, K. W. K. Yeung and S. C. Tjong, *Polymers*, 2016, **8**, 425–444.
28 J. Yang, Y. Xiao, C. Yang, S. Li, X. Qi and Y. J. Wang, *Eur. Polym. J.*, 2018, **98**, 375–383.
29 A. L. Myers and P. A. Monson, *Langmuir*, 2002, **18**, 10261–10273.
30 S. Zulfiqar, M. I. Sarwar and D. Mecerreyes, *Polym. Chem.*, 2015, **6**, 6435–6451.
31 M. J. Muldoon, S. N. V. K. Ali, J. L. Anderson, J. K. Dixon and J. F. Brennecke, *J. Phys. Chem. B*, 2007, **111**, 9001–9009.
32 G. Osei-Prempeh, H. J. Lehmler, S. E. Rankin and B. L. Knutson, *Ind. Eng. Chem. Res.*, 2011, **50**, 5510–5522.
33 A. P. Kharitonov and L. N. Kharitonova, *Pure Appl. Chem.*, 2009, **81**, 451–471.
34 A. Shahtalebi, M. Mar, K. Guerin and S. K. Bhatia, *Carbon*, 2016, **96**, 565–577.
35 R. G. Nicolas, F. Berube, M. Thommes, M. T. Janicke and F. Kleitz, *J. Phys. Chem. C*, 2017, **121**, 24505–24526.
36 S. J. McGurk, C. F. Martin, S. Brandani, M. B. Sweatman and X. Fan, *Appl. Energy*, 2017, **192**, 126–133.
37 M. Wang, J. Zhao, X. Wang, A. Liu and K. K. Gleason, *J. Mater. Chem. A*, 2017, **5**, 8860–8886.